Published in Tribology International 2010 Vol. 43, Issues 8 (2010) p. 1500-1507 http://dx.doi.org/10.1016/j.triboint.2010.02.010

# Interface roughness effect on friction map under fretting contact conditions

K.J. Kubiak, T.G. Mathia, S. Fouvry

[1] Laboratoire de Tribologie et Dynamique des Systèmes, CNRS UMR 5513, Ecole Centrale de Lyon, 36 Avenue Guy de Collongue, 69134 Ecully, France

*Corresponding author: krzysztof@kubiak.co.uk

**Abstract:**

In many industrial applications where fretting damage is observed in the contact (e.g. rotor/blade, electrical contacts, assembly joint, axe/wheel, clutch) the external loadings or geometry design cannot be changed. Therefore, the surface preparation and finishing process become essential to control and reduce the damage caused by fretting. In this paper, the authors present the experimental study of the initial surface roughness and machining process influence on fretting conditions in both partial and full sliding regimes. Surfaces prepared by milling and smooth abrasive polishing processes have been analysed. The influence of roughness on sliding behaviour and analysis of friction have been reported. Also, the contact pressure influence and qualitative analysis of fretting wear scar have been presented.

*Keywords: Fretting map, Surface roughness, Sliding regime, Texturation.*

**Nomenclature:**

$\delta$ - displacement (μm),

$\delta^*$ - displacement amplitude (μm),

$\delta_t$ - sliding transition displacement amplitude (μm),

$\Delta\delta$ - incremental step of displacement amplitude (μm),

P - normal force (N),

Q - tangential force (N),

$Q^*$ - tangential force amplitude (N),

$p_o$ - maximum Hertzian's contact pressure (MPa),

a – Hertzian's contact radius (μm),

N - number of fretting cycles,

$\Delta N$ - number of fretting cycles between the incremental steps of displacement,

$S_q$ - 3D surface root mean square (RMS) roughness (μm),

$S_a$ - 3D surface average roughness (μm),

$S_z$ - 3D surface peak-to-valley average maximum height (μm),

$S_t$ - 3D surface peak-to-valley maximum peak height (μm),

$\mu$ - coefficient of friction $Q^*/P$,

PS - partial slip (sliding condition regime),

FS - full sliding (sliding condition regime),

$\mu_t$ - coefficient of friction at the transition PS/FS,

$\mu_{stab}$ - stabilised coefficient of friction in FS regime,

$\sigma_{Y(0.2\%)}$ - yeld stress (MPa),

$\sigma_{UTS}$ - ultimate tensile stress (MPa),

E- elastic modulus (GPa),

## 1 Introduction

Fretting phenomenon is considered as a special damage process related to wear and cracking. Fretting occurs in the contact between two bodies subjected to the normal load and sliding induced by external cyclic forces or vibration. Depending on the relative displacement at the interface, Partial Slip or Full Sliding condition can be observed in the contact. In PS situation, the central zone of the contact, remains in stick condition, without the relative displacement and the external zone of contact is subjected to sliding (Fig. 1). In the FS condition, the entire area of contact is subjected to sliding (Fig. 1). Therefore, the fretting damage mode depends on sliding conditions, leading to cracking under PS and wear under FS condition [1]. Fretting is a dynamical process where sliding conditions and surface morphology of contacting materials can vary with time. In many industrial applications, it is not possible to control the fretting degradation process. Therefore, the initial design of such elements is the only way to prevent or to reduce the fretting phenomenon and surface damage. If it is not possible to modify the contact loading to reduce fretting degradation, the initial roughness could be optimised. Dulias et all. noted strong influence of surface roughness on sliding conditions [2]. However, relation between surface morphology and friction behaviour has been mainly studied in the mono-directional sliding [3] or in the FS conditions in order to evaluate the influence of roughness on wear behaviour [4]. In this paper, focus will be given on small amplitude, fretting sliding conditions. Under fretting and especially in the PS condition not much work has been published. Wong et all. [5] have reported influence of roughness on ceramics under mixed and hydrodynamic lubrication, a decreasing friction coefficient has been found for smoother surfaces. For aluminium alloy under dry fretting contact conditions Proudhon et all. [6] have noted influence of roughness where the rough surface tends to decrease the coefficient of friction at transition from PS to FS.

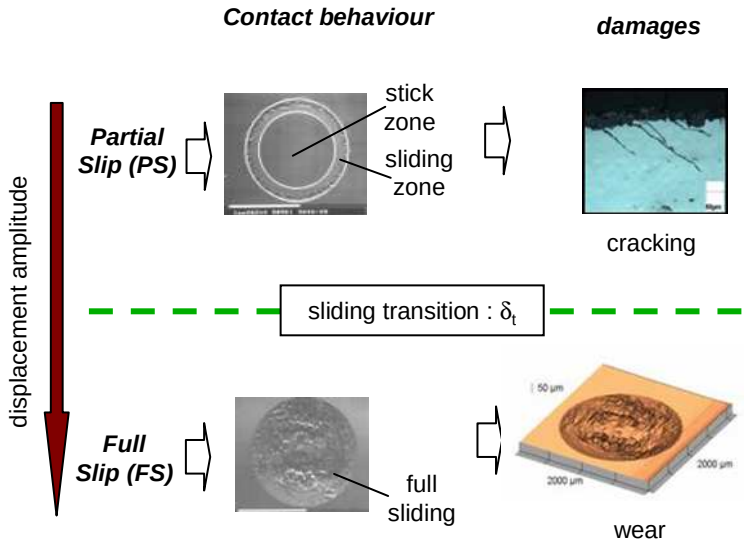


Fig. 1: Typical fretting damage observed under Partial Slip and Full Slip conditions [7].

To illustrate the transition between PS and FS the relationship between contact loading conditions (normal load, displacement amplitude, tangential load) and the sliding conditions (Partial Slip, Full Sliding) have to be considered. This relationship and observed damage phenomenon (cracking in PS and wear in FS) can be illustrated on the so-called Fretting Maps (FM). Firstly introduced by Vingsbo [8] the FM can present the running conditions (Running Conditions Fretting Map, RCFM, Fig. 2a) and material response (Material Response Fretting Map, MRFM, Fig. 2b).

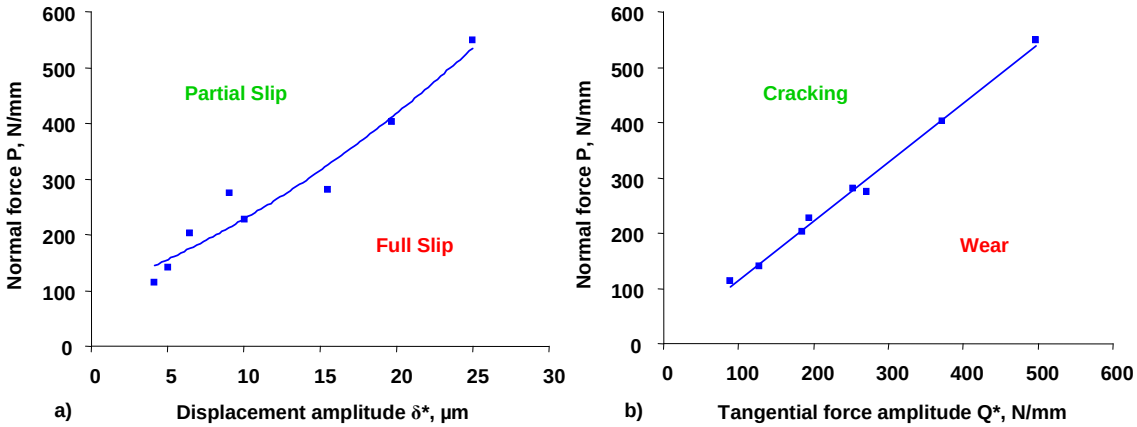


Fig. 2 Fretting maps: a) RCFM, b) MRFM, (AISI 1034, cylinder/plane configuration, R=40mm, normalised by cylinder axial contact length, N/mm) [9].

In PS condition where displacement is limited to external zone of contact (Fig. 1) surface roughness can influence local sliding condition, and generate local plastic deformation at contacting surface peaks. This lead to change in sliding behaviour and can cause uncontrolled damage. Therefore, better understanding of the surface roughness influence on fretting sliding phenomenon have a great interest for practical applications. This paper present the experimental results of initial surface roughness influence on fretting sliding conditions, to illustrate

this relationship fretting map concept have been used. Reported fretting map curves, plotted for surfaces with different initial roughness, demonstrate their influence on friction behaviour.

## 2 Experimental procedure

Fretting tests have been curried out using classical sphere/plane configuration, where the radius of sphere was 50 mm. Specific fretting device has been rigidly mounted on the universal fatigue machine [10]. Schematic diagram of fretting test equipment is presented in the Fig. 3.

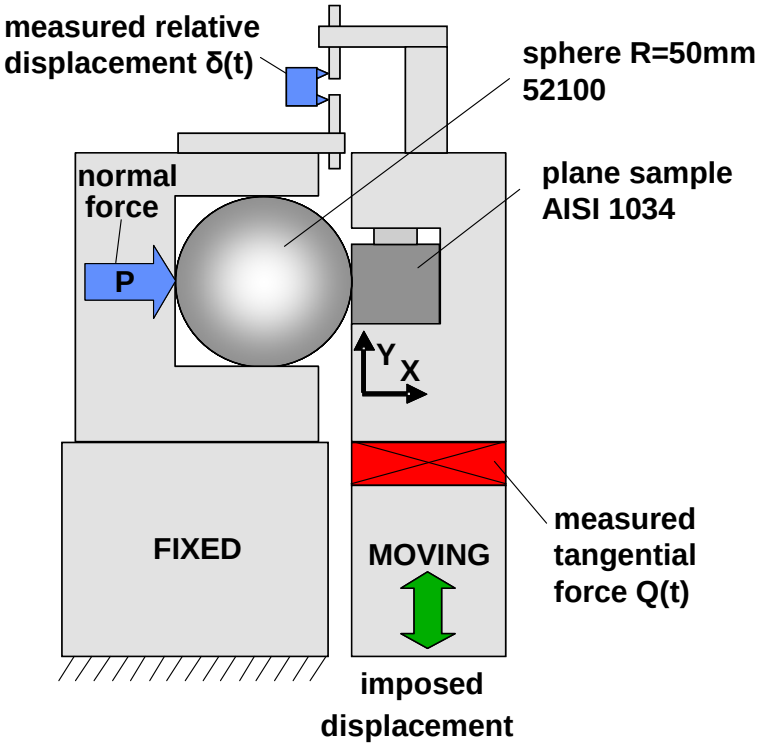


Fig. 3: Schematic diagram of fretting test device in sphere/plane configuration.

During the test, applied normal force P has been kept constant, sinusoidal displacement has been successively increased (see section 2.2). The normal force P, tangential force Q and relative displacement δ have been recorded. All experiments have been performed at displacement frequency of 20 Hz. Before the tests, all specimens have been cleaned in acetone and ethanol. Tests have been performed in ambient labolatory conditions at the temperature ~23ºC, and the relative humidity between 40 and 45%.

### *2.1 Studied materials*

One of the industrial applications where fretting problem is occurring is contact between the axe and wheel of the train. In this application, the important plastic deformation have been observed due to fitting process. Authors inspired by this application, have selected similar low carbon alloy AISI 1034 for the plane material. In order to reduce the plastic deformation in the contact, the AISI 52100 material has been used for the sphere

counterbody. Chemical composition and the mechanical properties of the studied materials are listed in the Table 1 and Table 2 respectively.

Table 1: Chemical composition of tested materials.

| Materials | | C | Mn | Cr | Ni | Ti | Cu | Si | P | S | Mo | V |
|---|---|---|---|---|---|---|---|---|---|---|---|---|
| AISI 1034 (plane) | max (%) | 0.38 | 1.2 | 0.3 | 0.3 | - | 0.3 | 0.5 | 0.02 | 0.02 | 0.08 | 0.06 |
| 5210 (sphere) | max (%) | 1.0 | 0.3 | 1.5 | 0.4 | 1.0 | 1.0 | 0.2 | 0.02 | 0.02 | 0.1 | 0.3 |

Table 2: Mechanical properties of tested materials.

| Materials | E (GPa) | Poisson ratio ν | $\sigma_{Y(0.2\%)}$ (MPa) | $\sigma_{UTS}$ (MPa) |
|---|---|---|---|---|
| AISI 1034 (plane) | 200 | 0.3 | 350 | 600 |
| 52100 (sphere) | 210 | 0.3 | 1700 | 2000 |

### *2.2 Incremental displacement method*

In PS condition, sliding displacement and dissipated in the interface energy (represented by hysteresis on graph Q=f(δ) so-called "fretting loop") are relatively low. Damage in the PS is usually limited to the external sliding zone of the contact. In FS condition, displacement amplitude and therefore energy dissipated at the contact are much higher. Sliding can be observed in all area of contact and high rate of wear damage occurs at interface. In order to prevent or reduce wear damage it is essential to know the sliding behaviour and transition between PS and FS (Fig. 4).

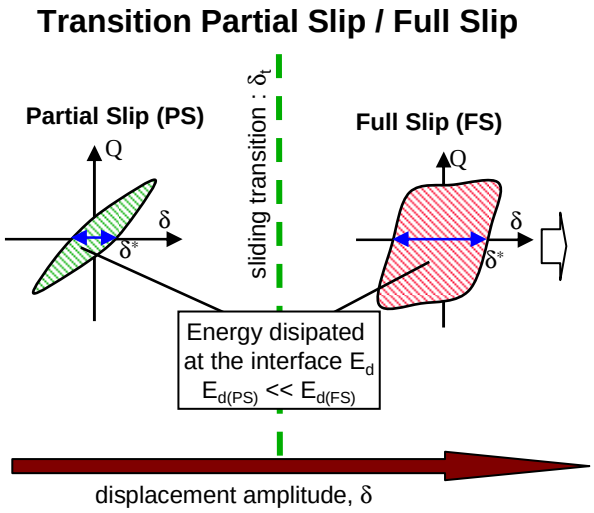


Fig. 4: Schematic diagram of transition between PS / FS and corresponding fretting loops.

To analyse this contact sliding behaviour in PS and in FS conditions, the incremental displacement method [11] has been applied. This method consist in successive increase of displacement amplitude from very small in PS to large displacement in FS conditions. The test start at displacement amplitude of $\delta^*$=1 µm and after each 1000 of

cycles the amplitude is increased by $\Delta\delta^*$=0.2 μm. The graphical representation of test method is presented in Fig. 5. The test duration is usually 200 000 cycles, hence the transition from PS to FS sliding conditions can be measured. Relevant parameters such as coefficient of friction (COF) at the transition PS/FS ($\mu_t$), relative contact sliding $\delta^*$ (calculated from fretting loop, as amplitude of sliding at Q=0 N, see Fig. 4) and COF in FS conditions ($\mu_{stab}$) have been calculated. Note that $\mu_{stab}$ correspond to the stabilized value of COF represented by the mean value of COF from the last 5000 of cycles, where $\mu_{stab}$ is expressed by:

$$\mu_{stab.} = \frac{1}{n}\left[\sum_{n}^{n-5000}\left(\frac{Q^*}{P}\right)\right] \qquad (1)$$

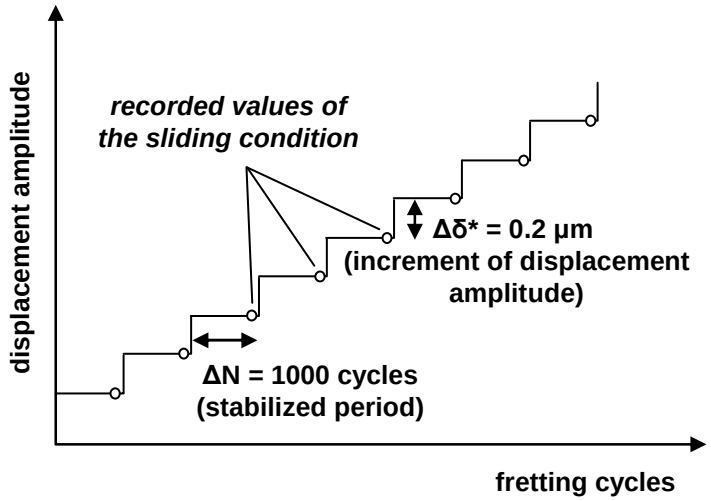


Fig. 5: Illustration of incremental displacement test method.

### *2.3 Surface morphologies*

Plane specimens have been machined into rectangular bars and the specific machining process has been applied on one of the surfaces in order to produce the morphologies with wide range of roughness values. After that, bars have been cut into small rectangular prisms (10x10x14 mm), hence, identical surface morphologies have been obtained on several specimens, moreover fretting traces are small and at least three tests can be curried out on the same specimen.

Any machining process has two main purposes: first is to obtain required shape and second is to obtain the functional surface by finishing process. However, there are no simple rules relating the manufacturing process, surface topography and specific properties of assembled interfaces [12, 13]. In this study two different machining processes have been used, milling and abrasive polishing, in order to analyse wide range of surface roughness parameters such as $S_a$ (surface average roughness), $S_q$ (surface root mean square roughness), $S_z$ (surface peak-to-valley average maximum height), $S_t$ - (surface peak-to-valley maximum peak height) and $R_{mr}$ (Relative material ratio of roughness profile). Manufactured surfaces present mono-directional, highly anisotropic textures orthogonally oriented to the sliding direction. Textured surfaces obtained by milling process are presented in Fig. 6. They have been machined with the same tool but with different machining parameters. Nevertheless, milling process can introduce residuals stress into the machined surface therefore, the plane

specimens have been tempered in 250ºC during 2 hours, in order to reduce the subsurface stresses after the machining process.

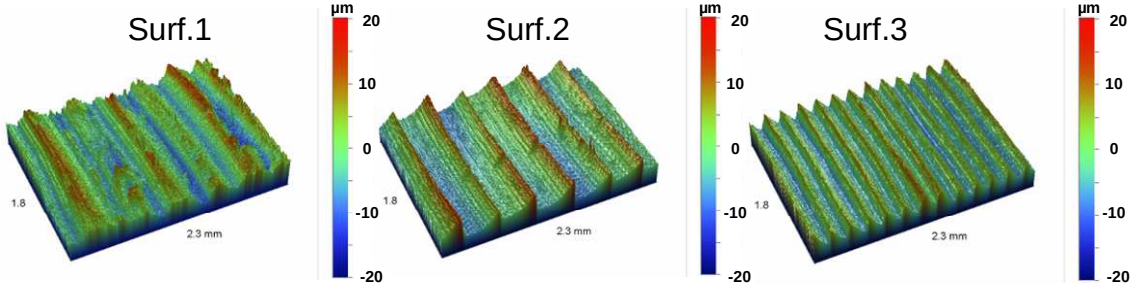


Fig. 6: 3D morphology images of initial surface roughness on plane specimens, prepared by milling process.

For smooth surfaces (Surf. 4-7) prepared by abrasive polishing process different grids of sand paper have been used, from 240 for rough (Surf.4) up to 4000 grid paper for mirror-polished surface (Surf.7). Morphologies of these surfaces are presented in Fig. 7.

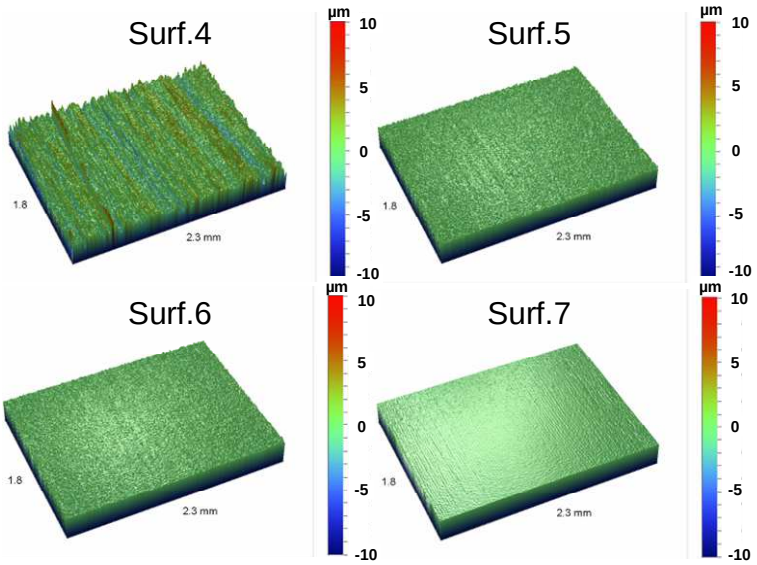


Fig. 7: 3D morphology images of initial surface roughness on plane specimens, prepared by abrasive polishing.

There are many different optical or tactile techniques, devoted to surface topography measurements. Suitable selection of these techniques depends mainly on horizontal (x,y) and vertical (z) resolution. Most tactile techniques are time-consuming [14]. In this study, the interferometric 3D profilometer (Veeco) has been used to measure and analyze the tested surfaces. Summary of surface machining processes and the most common surface roughness parameters is presented in Table 3.

Table 3: Parameters of initial surface roughness and machining processes.

| Plane Reference | Surface Preparation | $S_a$ (μm) | $S_q$ (μm) | $S_z$ (μm) | $S_t$ (μm) | $R_{mr}$ (%) 1 μm under the highest peak |
|---|---|---|---|---|---|---|
| Surf. 1 | milling-cutting | 4.15 | 5.11 | 35.05 | 39.54 | 1.68 |
| Surf. 2 | milling-cutting | 4.15 | 5.10 | 30.76 | 32.6 | 2.87 |
| Surf. 3 | milling-cutting | 3.66 | 4.31 | 27.56 | 29.35 | 4.52 |
| Surf. 4 | polishing-abrasion (240) | 1.52 | 2.00 | 27.00 | 39.09 | 5.51 |
| Surf. 5 | polishing-abrasion (800) | 0.32 | 0.45 | 6.41 | 8.41 | 8.67 |
| Surf. 6 | polishing-abrasion (1200) | 0.28 | 0.40 | 5.78 | 6.52 | 88.9 |
| Surf. 7 | polishing-abrasion (4000) | 0.09 | 0.11 | 1.02 | 1.29 | 100 |

## 3 Results and discussion

In present paper the experimental analysis of surface roughness influence on Fretting Map (FM) has been performed. Seven different surface morphologies have been tested, three were prepared by milling (Surf.1-3) and four prepared by abrasive polishing process (Surf.4-7). Therefore analysed range of surface roughness value is from $S_z$=1 μm to $S_z$=35 μm. To illustrate the roughness influence by using FM several values of contact pressures have been analysed. The following maximum Hertzian's contact pressure values have been selected $p_o$=500, 700, 900 and 1000 MPa where the initial Hertzian's radius contacts were a=350, 490, 630 and 700 μm respectively. Application of such pressures results in local plastic deformation but only in the central part of the contact (Fig. 1, Fig. 12 and Fig. 13) on plane specimens. However, plastic deformation can be partially accumulated by the rough surface asperities, as it was explained in detail in the paper [15]. In PS plastically deformed central zone of contact remains in stick condition and have less influence on friction behaviour and fretting wear damage process.

In order to optimize and to reduce the number of individual tests as well as to estimate the level of confidence of the reported results, the statistical approach of Design of Experiment (DOE) [16] has been applied. By using DOE the number of test needed for 4 pressures level and 7 surface morphologies can be reduced from 28 to 16, however for practical reasons additional repeated tests have been performed in order to estimate experimental incertitude limits which has been found to be at level of 8%. All 7 prepared surfaces have been tested for pressure level $p_o$=1000 MPa.

### *3.1 Friction analysis*

The incremental displacement method used in the present study is an efficient way to provide complete overview of friction behaviour in the PS and FS conditions, through the single experimental test. As presented in Fig. 5, successively increased displacement amplitude permits to establish the transition between PS and FS conditions. For sphere/plane contact configuration, this transition corresponds to the maximum value of COF ($\mu_t$) [17]. After

transition, all surface contact area is subjected to sliding. Wear process and creation of debris (third body) lead to decrease the COF in FS condition, until stabilized state ($\mu_{stab}$).

In the Fig. 8 the evolution of COF is plotted as a function of sliding distance amplitude. It can be noted that the initial surface roughness have strong influence on sliding behaviour and the COF at the transition ($\mu_t$). For the smooth surface (Surf.7) the value of $\mu_t$ is 1.05 which is 25% higher then for the rough surface (Surf.1), where $\mu_t$=0.75. Results of experimental analysis are listed in Table 4. The relevant surface roughness parameters, corresponding to tested surfaces can be found in Table 3.

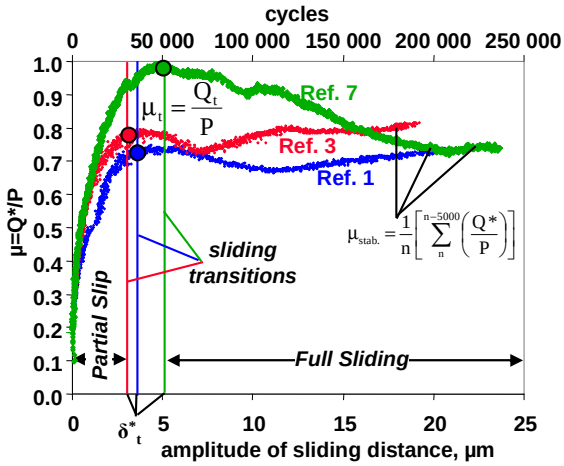


Fig. 8: Identification of sliding transition parameters, depending on surface roughness from incremental displacement method tests.

Table 4: Results of frictional and sliding parameters obtained by incremental displacement method (number of tests optimised by Design Of Experiment method).

| Test number | Hertzian's contact pressure [MPa] | Specimen Reference | $\delta_t$ [um] | $\mu_t$ | $\mu_{stab.}$ |
|---|---|---|---|---|---|
| 1 | 500 | Surf. 1 milling-cutting | 0.9 | 0.63 | 0.5 |
| 2 | 500 | Surf. 3 milling-cutting | 0.7 | 0.65 | 0.49 |
| 3 | 500 | Surf. 4 polishing-abrasion (240) | 0.4 | 0.703 | 0.52 |
| 4 | 500 | Surf. 7 polishing-abrasion (4000) | 0.6 | 0.816 | 0.577 |
| 5 | 700 | Surf. 1 milling-cutting | 1.2 | 0.71 | 0.66 |
| 6 | 700 | Surf. 3 milling-cutting | 1.3 | 0.73 | 0.65 |
| 7 | 700 | Surf. 4 polishing-abrasion (240) | 1.1 | 0.78 | 0.69 |
| 8 | 700 | Surf. 4 polishing-abrasion (240) | 1.3 | 0.79 | 0.66 |
| 9 | 700 | Surf. 4 polishing-abrasion (240) | 1.2 | 0.74 | 0.65 |
| 10 | 700 | Surf. 7 polishing-abrasion (4000) | 1.3 | 0.76 | 0.71 |
| 11 | 900 | Surf. 1 milling-cutting | 1.5 | 0.69 | 0.6 |
| 12 | 900 | Surf. 3 milling-cutting | 1.9 | 0.79 | 0.62 |
| 13 | 900 | Surf. 4 polishing-abrasion (240) | 2.7 | 0.77 | 0.71 |

| | | | | | |
|---|---|---|---|---|---|
| 14 | 900 | Surf. 7 polishing-abrasion (4000) | 2.8 | 0.91 | 0.74 |
| 15 | 1000 | Surf. 1 milling-cutting | 2.4 | 0.75 | 0.73 |
| 16 | 1000 | Surf. 2 milling-cutting | 3.0 | 0.81 | 0.79 |
| 17 | 1000 | Surf. 3 milling-cutting | 2.9 | 0.82 | 0.81 |
| 18 | 1000 | Surf. 4 polishing-abrasion (240) | 3.6 | 0.91 | 0.71 |
| 19 | 1000 | Surf. 5 polishing-abrasion (800) | 3.7 | 0.90 | 0.73 |
| 20 | 1000 | Surf. 6 polishing-abrasion (1200) | 3.4 | 0.89 | 0.75 |
| 21 | 1000 | Surf. 7 polishing-abrasion (4000) | 5.2 | 1.05 | 0.77 |

### *3.2 Influence of roughness on fretting sliding (Fretting Maps)*

Experimental analysis has been performed in the range of maximum Hertzian's contact pressure ($p_o$=500 - 1000 MPa), that allows to establish the Running Condition Fretting Map (Fig. 9) and two sliding regimes, PS and FS can be defined. It has been observed that amplitude of sliding distance at the transition between PS and FS is increasing with the normal load applied to contact. The significant influence of initial roughness on the transition can be noted for higher values of contact loading. For instance at contact pressure of $p_o$=1000 MPa, amplitude of sliding distance increases from 2.4 to 5.2 µm for Surf.1 and Surf.7 respectively. However, for lower contact loading the differences are much smaller, and for contact pressure of $p_o$=500 MPa the inverse situation can be observed, where the sliding amplitude at transition is bigger for rough surface (Surf. 1). To better understand this phenomenon additional investigation has to be performed in the range of lower contact loadings.

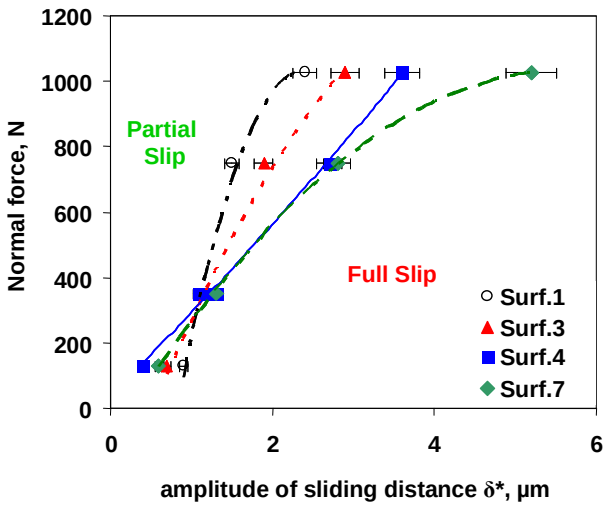


Fig. 9: Running Conditions Fretting Map (RCFM) for sphere/plane contact configuration and different initial surfaces roughness values.

Analysis of initial roughness influence on friction behaviour has been presented in Fig. 10. The significant increase in COF at transition PS/FS can be observed for smoother surfaces prepared by abrasive polishing (Fig. 10a). COF in the FS conditions remain quasi-constant within analyzed range of initial roughness ($S_z$=1 - 35 µm). This phenomenon can be explained by following hypothesis: in FS condition, entire area of contact is subjected to sliding and therefore to wear degradation process, which will affect the surface roughness and sliding

condition. Initial roughness will be changed or removed under FS condition, therefore initial roughness influence is limited to PS condition.

Analysis of sliding amplitude at transition PS/FS ($\delta^*_t$) demonstrate decrease of $\delta^*_t$ as a function of initial roughness ($S_z$). In order to prevent or delay the transition PS/FS, smoother surface finishing is required.

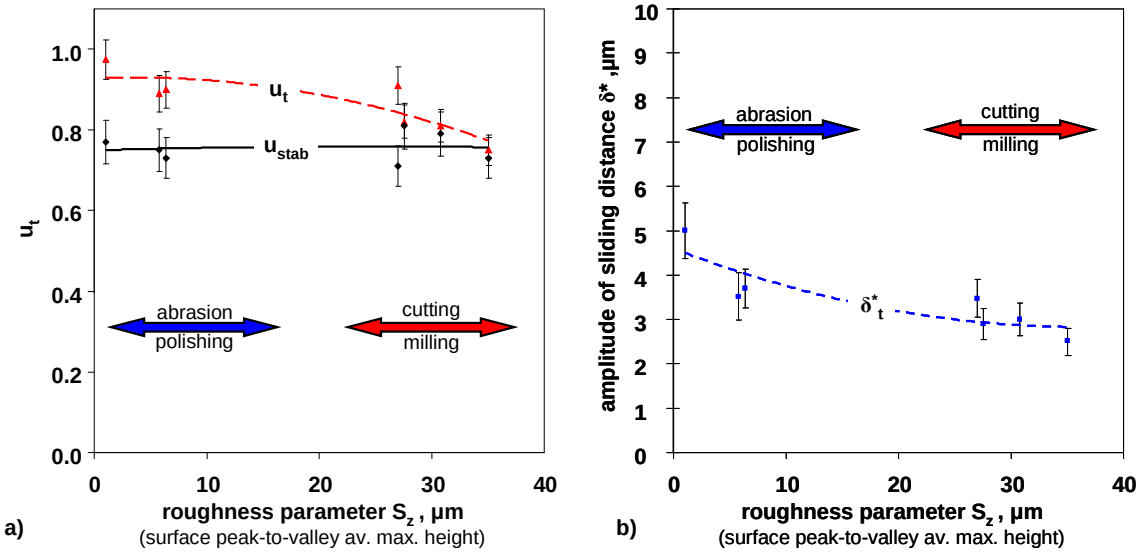


Fig. 10: Analysis of initial roughness influence $S_z$ on a) COF ($\mu_t$, $\mu_{stab}$) , b) sliding amplitude at transition PS/FS ($\delta^*_t$), for sphere/plane configuration at Hertzian's contact pressure $p_o$=1000 MPa.

### *3.3 Influence of contact pressure*

Analysis of normal load influence has been curried out in the range of Hertzian's pressure from $p_o$=500 to 1000 MPa. From the analysis of roughness and contact pressure presented in Fig. 11, it can be noted that for smooth surfaces and higher contact pressure, higher values of COF at the transition ($\mu_t$) can be observed. This phenomenon can be explained by the following hypothesis: for the specimen with smaller roughness (Surf.7), local area of the contact between sphere and plane specimens is bigger than for the specimen with higher roughness (Surf. 1). It is confirmed by analysis of relative material ratio curve that describes the percentage of material which is traversed by a cut at a certain level located with respect to the highest point on the profile (1 µm under highest peak). This approach is known as the Abbott-Firestone curve. For smooth surface (Surf. 6) relative material ratio of profile is $R_{mr}$=88.9 % while for rough profile (Surf. 1) $R_{mr}$=1.68 % (Table 3). During the test incrementally increasing amplitude of displacement provokes the transition from PS to FS, this transition corresponds to relative sliding and plastic deformation in the entire contact [18] as it has been pointed out previously. Therefore, during the transition between PS/FS, for specimens with small surface roughness (bigger local contact area) the value of the tangential force due to local plastic deformation, will be higher than for the specimens with high surface roughness, were the effective contact area is smaller (Fig. 11).

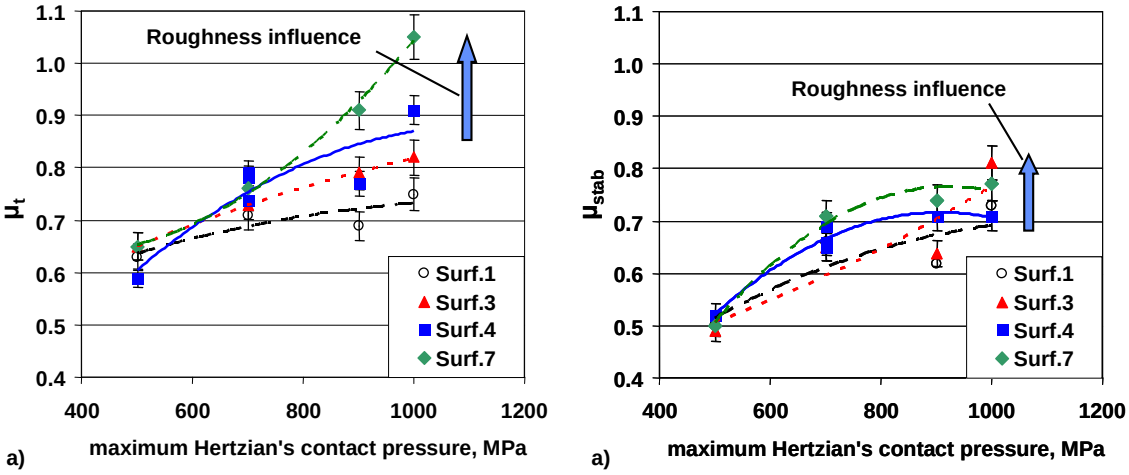


Fig. 11: Influence of initial roughness and contact pressure on friction behaviour ($\mu_t$ ,$\mu_{stab}$).

For all tested surfaces, increase of COF at the transition as well as in the FS conditions can be observed (Fig. 11). The analyse of plastic deformation in the interface can help in understanding this tendency. The plasticity threshold for AISI 1034 alloy is $\sigma_{Y(0.2\%)}$=350 MPa, therefore for the studied pressures the plastic deformation takes place in the plane counter body. The extension of contact due to plastic deformation in the central zone of contact, tends to increase value of COF at the transition PS/FS ($\mu_t$) and under FS condition ($\mu_{stab}$) due to larger area of contact and therefore higher number of local peaks deformed during sliding. Once again it can be noted that the initial surface roughness value have strong influence on COF at the transition ($\mu_t$) and especially for higher values of pressure ($p_o$=1000 MPa) where roughness increase COF at the transition PS/FS, $\mu_t$ (Fig. 11).

### *3.4 Fretting wear scars analysis*

In incremental displacement method (section 2.2) number of cycles in PS is different for each test. Therefore, wear of material observed in FS condition is depending on the sliding history in PS regime. PS period will be longer if transition PS/FS is observed for larger value of sliding amplitude at transition. Number of cycles in FS is also different for each test, that is why the direct comparison and quantitative wear analysis are not possible. Hence, the wear analysis is limited to the qualitative description only. In Fig. 12 and Fig. 13 fretting wear scars and 3D morphologies are presented. High deformation of fretting wear scars and plastically displaced material can be observed in both cases. Under dry friction conditions, where value of COF is high, the amount of energy dissipated at the interface, is important. Analysis of the scar morphology indicates degradation of the surface by wear process in the central zone and plastic deformations in the external zone [18]. Scar morphologies have directional character conforming to fretting sliding direction.

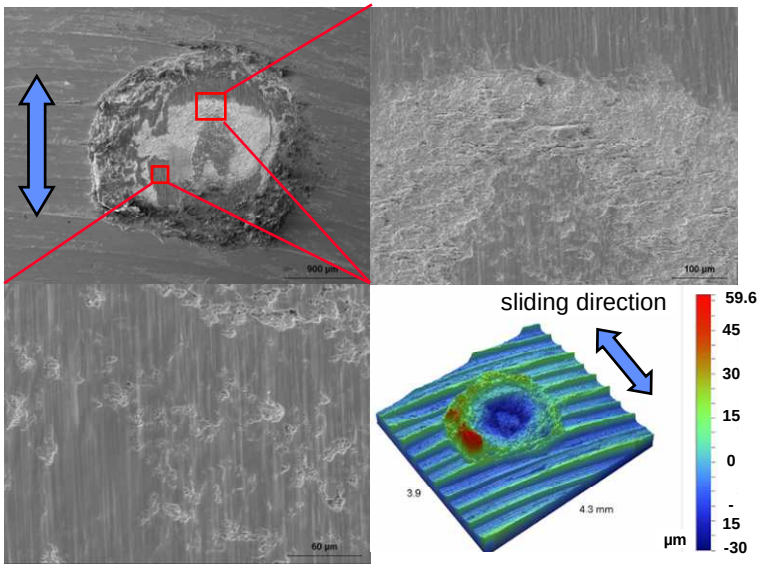


Fig. 12: SEM observations and 3D morphology of wear scar at milled surface (Surf.2).

On plane specimens, the central zone where the material has been removed due to wear process and the external zone where friction marks and plastic deformations can be observed are characterized by different surface roughness. For central zone $S_a$=2.7 µm and for external zone $S_a$=1.66 µm. It can be noted that in the central zone where the contact pressure is higher the wear rate is also higher and as a result U shape crater has been created in the plane specimen. From 3D morphology, wear volume and plastically deformed volume of material can be measured. The volume of plastically deformed external zone in case of rough surface (Surf.1), where the plastic deformation was the most important, is about 11% of the volume removed by wear. Hence, the dominant mode of degradation of the surface is the wear process and the plastic deformation in the contact plays the secondary role. On sphere specimens, observed fretting wear scars have been characterised by very low degradation in comparison with plane specimens.

However, additional investigation curried out in FS regime only is needed to analyse roughness influence on wear rate observed under fretting condition. Also, the role of plasticity should be further investigated, for instance by an elasto-plastic Finit Elements Analysis.

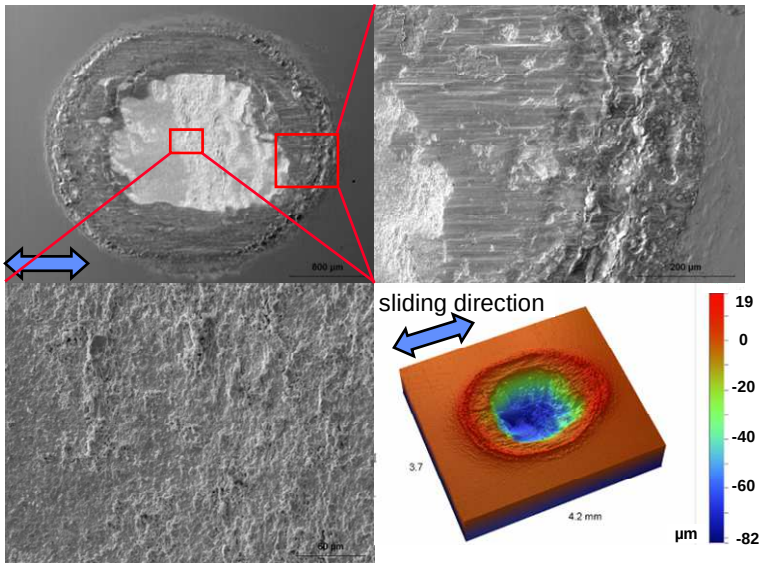


Fig. 13: SEM observations and 3D morphology of wear scar at polished surface (Surf.7).

Experimental results presented in this study attempt to establish the new approach to the fretting friction and sliding problems analysis. The authors attempt to demonstrate the influence of surface roughness and surface finishing process on friction behaviour under fretting conditions. Increase of coefficient of friction at the transition between partial slip and gross lip regime has been reported (Fig. 10a).

## 4 Conclusions

Significant influence of initial surface roughness on coefficient of friction (COF) at the transition between Partial Slip (PS) and Full Sliding (FS) has been reported. The selection of manufacturing process is essential for final application of assembled joints subjected to the fretting loading conditions. The following conclusions can be drawn from the presented experimental study:

- The initial roughness and therefore topographical parameters, and machining process have a strong influence on the COF ($\mu_t$) at the transition between PS and FS, for lower values of surface roughness increase of COF can be observed (Fig. 8 and Fig. 10a),
- For all tested surface morphologies COF at the transition $\mu_t$ is higher than $\mu_{stab}$, for the abrasive polished surfaces the differences are greater (Fig. 10a),
- For the polished surfaces one can observe strong influence of initial surface roughness value on the ($\mu_t$) while ($\mu_{stab}$) remains quite stable (Fig. 10a),
- Sliding amplitude $\delta^*_t$ (Fig. 9), COF $\mu_t$ (Fig. 11a) and $\mu_{stab}$ (Fig. 11b) are increasing as a function of maximum Hertzian's contact pressure,
- The two zones of different degradation mode can be distinguished in contact area: central zone of wear damage and external zone of the friction and plastic deformation (Fig. 12 and Fig. 13).

## 5 Acknowledgements

The authors would like to thanks Mr Jean-Michel Vernet for technical advice on cutting and abrasive machining and manufacturing of model surfaces for experimental investigation.

## 6 References

[1] K. Kubiak, S. Fouvry, A.M. Marechal, A practical methodology to select fretting palliatives: Application to shot peening, hard chromium and WC-Co coatings, Wear 259 (2005) p. 367–376.
[2] U. Dulias, L. Fang, K.H. Zum Gahr, Effect of surface roughness of self-mated alumina on friction and wear in isooctane-lubricated reciprocating sliding contact, Wear (2002), Vol. 252, Issues 3-4, p. 351-358.
[3] D.J.W. Barrell, M. Priest, The interaction of wear rate and friction with surface roughness for a lubricated sliding contact, Tribology and Interface Engineering Series, Vol. 43 (2003), p. 807-814.
[4] C.Q. Yuan, Z. Peng, X.P. Yan, X.C. Zhou, Surface roughness evolutions in sliding wear process, Wear 265 (2008) p. 341–348.
[5] H-C. Wong, N. Umehara, K. Kato, The effect of surface roughness on friction of ceramics sliding in water, Wear 218, (1998), p. 237-243.
[6] H. Proudhon, et all, A fretting crack initiation prediction taking into account the surface roughness and the crack nucleation process volume, International Journal of Fatigue 27 (2005) p. 569–579.
[7]K. Kubiak, S. Fouvry, B.G. Wendler, Comparison of shot peening and nitriding surface treatments under complex fretting loadings, Materials Science Forum, 513 (2006) p. 105-118.
[8] O. Vingsbo, S. Söderberg, On fretting maps, Wear 126 (1988) p. 137–147.
[9] K. Kubiak, Quantification de la fissuration d'un contact soumis a des sollicitations complexes en Fretting wear et fretting fatigue, PhD thesis No. 2006-30 Ecole Centrale de Lyon.
[10] K. Kubiak, S. Fouvry, A.M. Marechal, J-M. Vernet, Behaviour of shot peening combined with WC–Co HVOF coating undercomplex fretting wear and fretting fatigue loading conditions, Surface & Coatings Technology 201 (2006) p. 4323–4328.
[11] Voisin J. M., Vannes A. B., Vincent L., Daviot J., Giraud B., "Analysis of a tube-grid oscillatory contact: methodology for the selection of superficial treatments", Wear 181-183 (1995) p. 826-832.
[12]Stout KJ, Blunt L, Dong WP, Mainsah E, Luo N, Mathia T, Sullivan PJ, Zahouani H. Development of methods for characterisation of roughness in three dimensions. London, UK: Penton Press; 2000. ISBN: 1857180232.
[13] T.G. Mathia, F. Louis, G. Maeder, D. Mairey, Relationships between surfaces states, finishing processes and engineering properties, Wear 83 (1982), p. 241-250.
[14] T.G. Mathia, H. Zahouani, J. Rousseau, J. C. Le Bosse, Functional significance of different techniques for surface morphology measurements, Int. J. Mach. Tools Manufact. Vol. 35. N° 2 (1995), p. 195 – 202.
[15] H. Zahouani, T.G. Mathia, A. Guinet, Evolution of 3D morphology surface's motifs in plastic contact, Tribologia - Finish, Journal of Tribology Vol. 11/1992 N° 4 p 45-50, 1992
[16] A. Han et all, Study and evaluation of fretting critical slip conditions by applying the design of experiments method, Wear 261 (2006) 1080–1086.
[17] S. Fouvry, L. Vincent and P. Kapsa, Quantification of fretting damage, Wear Vol. 200, Issues 1-2 (1996) p. 186-205.
[18] H. Zahouani, T.G. Mathia, J. Rousseau, Geomorphologic and Fractal Approaches in Contact Mechanics, Case of Plastic Deformation, Contact Mechanics, Plenum Publishing Corporation (1995) p. 299-304.